Title

Measuring Absolute Membrane Potential Across Space and Time

Journal

Annual Review of Biophysics, 50(1)

ISSN

1936-122X

Authors

Lazzari-Dean, Julia R
Gest, Anneliese MM
Miller, Evan W

Publication Date

2021-05-06

DOI

10.1146/annurev-biophys-062920-063555

Peer reviewed

Published in final edited form as:

Annu Rev Biophys. 2021 May 06; 50: 447–468. doi:10.1146/annurev-biophys-062920-063555.

Measuring Absolute Membrane Potential Across Space and Time

Julia R. Lazzari-Dean[1], **Anneliese M.M. Gest**[1], **Evan W. Miller**[1,2,3]

[1]Department of Chemistry, University of California, Berkeley, California 94720, USA

[2]Department of Molecular and Cell Biology, University of California, Berkeley, California 94720, USA

[3]Helen Wills Neuroscience Institute, University of California, Berkeley, California 94720, USA

Abstract

Membrane potential (V_{mem}) is a fundamental biophysical signal present in all cells. V_{mem} signals range in time from milliseconds to days, and they span lengths from microns to centimeters. V_{mem} affects many cellular processes, ranging from neurotransmitter release to cell cycle control to tissue patterning. However, existing tools are not suitable for V_{mem} quantification in many of these areas. In this review, we outline the diverse biology of V_{mem}, drafting a wish list of features for a V_{mem} sensing platform. We then use these guidelines to discuss electrode-based and optical platforms for interrogating V_{mem}. On the one hand, electrode-based strategies exhibit excellent quantification but are most effective in short-term, cellular recordings. On the other hand, optical strategies provide easier access to diverse samples but generally only detect relative changes in V_{mem}. By combining the respective strengths of these technologies, recent advances in optical quantification of absolute V_{mem} enable new inquiries into V_{mem} biology.

Keywords

microscopy; fluorescence; membrane potential; electrophysiology; fluorescence lifetime; quantitative imaging

1. INTRODUCTION

Membrane potential (V_{mem}), or voltage across a lipid bilayer, is ubiquitous in biology. In electrically excitable cells such as neurons and cardiomyocytes, millisecond V_{mem} fluctuations cause release of neurotransmitters and contraction. Both excitable and nonexcitable cells exhibit V_{mem} signals, which vary over timespans of seconds to days. Furthermore, an estimated 10–50% of the cellular energy budget goes to maintain V_{mem}, even in nonexcitable cells (96). Given this large energy expenditure, the functions of V_{mem} span far beyond excitable electrical activity in the brain or heart (2); recent work has linked V_{mem} to cell proliferation (26, 42), differentiation (25, 104), and tissue patterning (64).

jldean@berkeley.edu, evanwmiller@berkeley.edu.

Membrane potential (V_{mem}):

a voltage across a membrane, arising from differences in ion concentration on either side

V_{mem} results from differences in ion concentration across a semipermeable membrane. Although this phenomenon is best studied with respect to the plasma membrane of mammalian cells, any selectively permeable membrane can maintain a voltage. For example, voltages in bacterial communities (58, 60, 89) and across organelle membranes (20, 124) also have signaling roles. Unless otherwise indicated, we use the term V_{mem} to indicate the plasma membrane potential between the cytosol and the extracellular space. In addition, we use absolute V_{mem} to indicate the value of the membrane potential in millivolts, rather than a relative measure of changes in V_{mem}.

Absolute V_{mem}:

the value of V_{mem} in mV units; this term is used to differentiate between V_{mem} recording techniques that can quantify V_{mem} and those that can only track relative changes

V_{mem} is inherently a system-level property, determined by an array of ion channels and pumps and sensed by diverse cellular components. In mammalian cells, the primary ions involved in generating V_{mem} are Na^+ and K^+ (Figure 1a), but many other species (including Cl^-, Ca^{2+}, H^+, and organic anions) play a role. Within the cellular V_{mem} response, voltage-gated ion channels are the best-documented class of voltage-sensitive proteins; these channels transduce V_{mem} changes into additional ionic currents or fluctuations in the second messenger Ca^{2+}. Nevertheless, all membrane-localized proteins experience V_{mem}, and more of these proteins may be sensitive to V_{mem} than was previously thought. Evidence of V_{mem} sensitivity exists for various membrane components (121), including phosphatases (80), G protein–coupled receptors (92, 93), and the membrane organization itself (123). For most systems, we have an incomplete understanding of both the determinants of V_{mem} and the factors that respond to V_{mem}.

These gaps in our understanding are largely attributable to limitations in the existing V_{mem} recording toolkit, as most V_{mem} recording strategies are only tractable in a small subset of biological samples. In particular, strategies to record absolute V_{mem} and absolute V_{mem} changes (i.e., to document that V_{mem} depolarized by 20 mV) are unavailable in many systems (Figure 1b). To better understand necessary features of V_{mem} recording strategies, we first summarize known V_{mem} signaling pathways and build a wish list of features for an optimized V_{mem} reporter. We then turn our focus to the two primary approaches for recording V_{mem}: electrodes and fluorescent sensors. We review recent progress in V_{mem} sensing platforms and highlight areas where development of new tools would facilitate discovery.

2. MEMBRANE POTENTIAL SIGNALING ACROSS TIME AND SPACE

V_{mem} signaling is most extensively studied in excitable tissue, where rapid changes in cellular V_{mem} transmit information. However, important V_{mem} signals also occur across

minutes, hours, and days(2). Similarly, as a spatial signal, V_{mem} is canonically treated as cell autonomous and uniform in spherical model cells. Nevertheless, V_{mem} can be compartmentalized subcellularly (20, 30, 120, 124) and delocalized across tissues (21, 69, 76, 95). In this section, we break down V_{mem} signals into three length scales: cellular, subcellular, and tissue. From there, we enumerate the unique challenges that each scale brings for V_{mem} measurement.

2.1. Cellular Membrane Potentials: Action Potentials, Cell Cycle Control, Etc.

The many ion gradients across the plasma membrane create a cellular V_{mem}, which is generally assumed to be uniform across a cell due to free diffusion of ions within the cytosol. Many cellular V_{mem} events are short-lived; their quantification requires both high temporal resolution and high voltage resolution. An important fast V_{mem} signal is the action potential (AP) in excitable cells. APs in mammalian neurons typically last a few milliseconds, involving a rapid depolarization of approximately 100 mV followed by rapid hyperpolarization back to the resting V_{mem} (8). Many aspects of APs have important cellular effects, including waveform, frequency, and V_{mem} (AP amplitude, as well as initial and final absolute V_{mem}) (8). V_{mem} recording platforms have been engineered with the goal of recapitulating AP waveform and frequency, and modern versions of both electrode-based and optical strategies reflect excellent progress toward this end (14, 57, 77, 115, 116). However, options for recording AP amplitude or absolute V_{mem} are more limited (see below).

Action potential (AP):

a rapid, all-or-nothing V_{mem} signal in excitable cells that results from the activity of V_{mem}-sensitive ion channels

To extend recordings from milliseconds to minutes, hours, or days, two new requirements emerge. First, the V_{mem} recording technique must be stable over the relevant timeframe, displaying no artefactual, V_{mem}-independent changes in signal. Second, it must be noninvasive, with cellular processes continuing normally despite chronic observation. With existing tools, V_{mem} recordings on timescales longer than minutes are challenging and are infrequently attempted. As a result, we have an incomplete picture of what V_{mem} changes occur and little clarity regarding their effects. Nevertheless, it is evident that slower changes in V_{mem} are pleiotropic signals with important cellular roles. In neuroscience, for example, the resting V_{mem} of neurons influences the propensity to fire APs. Furthermore, neuronal resting V_{mem} changes in association with—and perhaps also regulates—diverse processes, including cellular metabolism (97) and circadian rhythm (63). In addition, V_{mem} appears to hyperpolarize during neuronal development and differentiation, although the magnitude of the observed changes varies drastically with the measurement technique used (48, 75, 105).

Furthermore, non-excitable cells also show V_{mem} changes on long timescales, often broadly related to growth. For example, V_{mem} changes associated with progression from the G1 to the S phase of the cell cycle have been documented in various cell lines (6, 108, 111), and acute epidermal growth factor receptor activation can be accompanied by a V_{mem} signal (59,

71, 86). In a disease context, cancer cells may be generally more depolarized than their nontransformed counterparts, implying that V_{mem} modulation may offer selective growth advantages (117). Nevertheless, because current techniques cannot monitor absolute V_{mem} on the same cell over hours to days, we lack a road map of V_{mem} throughout the cell cycle or in growth signaling.

2.2. Subcellular Membrane Potentials: Organelles and Membrane Compartmentalization

Because V_{mem} originates from ion concentration gradients, subcellular V_{mem} differences can only exist in areas of electrical compartmentalization, where diffusion is regionally restricted. Partial compartmentalization produces transient or metastable local differences in V_{mem}. To study subcellular V_{mem} differences, a technique requires exquisite spatial resolution, as well as access to subcellular structures without damaging them. Isolating the V_{mem} of a subcellular compartment from the cellular V_{mem} (which may be larger in magnitude and certainly occupies a larger region of space) is particularly challenging. However, direct evidence for subcellular V_{mem} differences exists, along with a preponderance of indirect evidence that V_{mem} is locally regulated in membrane-bound compartments.

Electrical compartmentalization:

a restriction on ionic flow that allows for local differences in ion concentration and V_{mem}

Electrical compartmentalization occurs where the plasma membrane forms compartmentalized processes, and the longevity of localized V_{mem} signals is determined by the resistance to ion flow in and out of the compartment. Transient subcellular V_{mem} signals occur in neurons, as voltage waveforms are transmitted and processed by dendrites (102) and the axon initial segment (53). Because these electrical compartments have nearly free ionic flow with other parts of the cell, the signals are fleeting. Visualization of dendritic computation and AP propagation requires exceptional temporal resolution, with recording rates often exceeding 10 kHz (9). Longer-lived subcellular differences likely exist in the micron-scale dendritic spines, insulated by high-resistance bottlenecks between the spine and the dendrite. Mounting evidence suggests that spine V_{mem} can be electrically distinct from the rest of the neuron, and its role in learning and memory is an area of active study (37, 120). In non-excitable cells, V_{mem} compartmentalization at the plasma membrane has yet to be conclusively shown. Nevertheless, the subcellular enrichment of particular ion channels in primary cilia (30, 99) and filopodia (44) suggests that nonuniform plasma membrane V_{mem} is likely.

Organellar membranes also offer an opportunity for ionic, and therefore V_{mem}, compartmentalization. Organellar electrode-based recordings are both invasive and challenging, as they often involve rupturing the plasma membrane. Nevertheless, through labor-intensive experimental efforts, we have some direct evidence for V_{mem} signals in organelles. For example, the mitochondrial V_{mem} (and H^+ gradient) is required for successful oxidative phosphorylation (124), and depolarized mitochondrial V_{mem}, as well as defective oxidative phosphorylation, is associated with neurodegenerative diseases (47). The

lysosome contains excitable channels (20), and the endoplasmic reticulum V_{mem} has been reported to respond to cellular V_{mem} (90). Furthermore, where direct recordings have not been made, proteomic and transcriptomic studies of organellar channels and transporters imply complex physiology (114), and improved methods tailored to the unique constraints of these subcellular systems are of great interest.

2.3. Membrane Potentials in Tissue: Long-Range Interactions and Delocalization

At the other extreme of the length scale, V_{mem} carries information via long-range interactions in tissues. Direct experimental interrogation of V_{mem} in tissue requires throughput and multiplexed measurement across many cells simultaneously, as well as the ability to measure in situ. Electrical communication over distances is facilitated by synaptic transmission, as well as by gap junctions. In the brain, neurons do not act in isolation, but instead form circuits (5, 13); understanding behavior requires simultaneous V_{mem} mapping across many cells. Beyond neural circuits, V_{mem} can be delocalized across tissues via gap junctions, which allow free flow of ions and many small molecules between cells. Early studies of electrical coupling and gap junctions were performed in the *Drosophila* salivary gland, where resistance to current flow between cells is only slightly higher than the resistance to flow within cells (69). Since then, gap junctions have been found to be ubiquitous, with dysfunction connected to various diseases (109). Gap junctions also enable rapid exchange of V_{mem} information across tissues, as in the synchronous electrical signaling in the heart (95).

Electrical coupling via gap junctions not only enables transmission of V_{mem} signals across a population of cells, but also inextricably links V_{mem} between coupled cells. Despite this, many observations about cellular V_{mem} signaling are made on isolated cells in culture. For epithelial cells that exist in vivo as a tightly coupled tissue, this is an artificial electrical state. What happens to the surrounding tissue when an individual cell changes its V_{mem} throughout the cell cycle or as a response to growth factor signaling? It remains unclear how and to what extent cell-autonomous V_{mem} signals discovered in isolated cells will translate into tissues. Theoretical studies suggest that, in some conditions, stable and metastable electrical patterning is possible, but it is highly dependent on the electrical coupling in the tissue (22, 23). These results imply that V_{mem} signals are accompanied—or at least modulated—by dynamic regulation of cell–cell coupling. Although some progress has been made toward direct visualization of V_{mem} distributions in tissue (21, 76), such measurements are largely unexplored.

Taken together, diverse biological questions necessitate a noninvasive, multiplexed, in situ V_{mem} platform with excellent spatiotemporal and voltage resolution. Throughput and technical ease of use of the platform are also important, as they enable top-down profiling experiments that can help elucidate V_{mem} signaling networks. Of the array of methods available today, no single approach possesses all of these characteristics (Tables 1 and 2). Indeed, more realistically, a toolkit of recording strategies will be required to fully interrogate V_{mem}. Below, we discuss the performance of existing V_{mem} measurement techniques, with an eye toward their ability to report V_{mem} across space and time.

3. ELECTRODE-BASED APPROACHES FOR RECORDING ABSOLUTE MEMBRANE POTENTIAL

Electrode-based techniques are the gold standard for recording V_{mem}, ion channel properties, and electrical currents in cells. Three primary configurations are used in cellular V_{mem} recordings: whole-cell patch clamp, cell attached, and perforated patch (Figure 2). All three can quantify absolute V_{mem} with excellent temporal resolution, but they suffer from high invasiveness, instability over time, low throughput, and poor spatial resolution (Table 1).

Whole-cell patch clamp:

a direct, electrode-based technique for recording V_{mem} in which physical contact is established between an electrode and the inside of a cell

3.1. Intracellular Recordings of Absolute Membrane Potential

In intracellular recording, V_{mem} is determined from the difference between a recording electrode in the cytosol and a reference electrode in the extracellular solution. More detailed treatment of the many capabilities of intracellular recording can be found elsewhere (14); we focus only on V_{mem} measurement. Two main types of intracellular recordings exist: sharp electrode and whole-cell recordings. Sharp microelectrodes possess very fine tips and high tip resistances, which produce a variable tip potential and a V_{mem} artifact on the order of tens of millivolts (14, 65). Furthermore, they create a leak in the cell of interest, producing artificially depolarized apparent V_{mem} and altered input resistance (65, 101). Although sharp electrode recordings are still in use in certain in vivo preparations, they have largely been replaced by intracellular recordings in the whole-cell configuration. Whole-cell intracellular recordings use much larger patch electrodes with lower tip potentials; such electrodes can be sealed onto the cell with less damage than sharp electrodes (100). Whole-cell recordings can also provide higher-resolution information about the particular ions and types of channels involved in setting V_{mem}.

Intracellular recording provides a direct, in situ measurement of V_{mem} with sub-mV precision and excellent temporal resolution, but it suffers from a variety of drawbacks. First, the whole-cell patch is highly invasive and disrupts the very processes under investigation. By dialyzing the cytosol with electrode internal solution, whole-cell patch clamp washes out soluble signaling factors (14, 49, 73). In addition, physical contact with the electrode can activate mechanosensitive channels and signal transduction pathways (70, 112), introducing further artifacts. With respect to the measurement itself, leaks in the seal between the recording electrode and the membrane can produce errors in recorded V_{mem} (105). More subtly, an electrode has poor spatial resolution, reporting V_{mem} at a point of contact that may or may not reflect other parts of the cell or tissue. For complex membrane structures or electrically coupled tissues, this space clamp error renders the effective recording area unknown (7, 110). For subcellular recordings, electrode-based strategies struggle to physically access subcellular compartments, as the size of the electrode tip provides a lower bound on the size of structures that can be interrogated (30, 37). Furthermore, intracellular

recordings are challenging to execute. Attempting each whole-cell recording takes an expert researcher or specialized robot 5–10 minutes, with a 10–30% success rate for these efforts (38, 52, 103). While in situ automated patch systems have reduced the need for human expertise and labor, they still do not achieve high throughput or multiplexing. Therefore, recording across many cells in the same tissue is nearly impossible, as is cataloging V_{mem} subpopulations over many cells.

3.2. Reducing Invasiveness: Cell-Attached and Perforated Patch Configurations

To mitigate the washout of soluble factors associated with whole-cell recording, V_{mem} must be measured without disrupting the plasma membrane. This is possible in the cell-attached configuration, in which an extracellular patch electrode is sealed onto the cell without rupturing the membrane. If the membrane resistance is approximately 100-fold lower than the seal resistance, then the voltage across the small membrane region under the pipette will reflect cellular V_{mem} with reasonable accuracy (87). Alternatively, if the channel composition and electrical properties are known in the cells of interest, then the reversal potential of these channels (determined in the cell-attached configuration) can also be used to infer V_{mem}. Such techniques have been demonstrated with the K^+ reversal potential in hippocampal interneurons (106), as well as the NMDA reversal potential in hippocampal CA3 neurons (105). However, this strategy is difficult to extend, as it requires detailed knowledge of the inventory and behavior of channels in the specific system of interest.

Cell-attached configuration:

an electrophysiological configuration where an electrode is sealed onto the membrane of a cell but the membrane is not ruptured

Perforated patch recordings offer a more general solution to reduce invasiveness of whole-cell recordings (40, 66). In perforated patch, an ionophore placed in the pipette internal solution allows ions to cross the membrane without completely disrupting it, thereby electrically connecting the cytosol with the pipette solution. Because the membrane remains impermeable to the diffusion of larger molecules, perforated patch recording can last over an hour without run-down of relevant cytosolic factors (40, 54).

Ionophore:

a molecule that can bind specific ions and diffuse across membranes, equalizing the electrochemical gradient for that ion

3.3. Engineering Electrodes for Improved Performance

Efforts to improve electrode-based recordings have also turned to the electrodes themselves, where recent developments have reduced invasiveness and improved throughput of electrode-based recordings. Below, we highlight two advances in electrode design: planar patch clamp and nanoscale electrodes.

3.3.1. Planar patch clamp.—With the development of low-noise arrays of patch electrodes (32), commercial planar patch clamp systems can now perform simultaneous, automated electrophysiological experiments in 384- or 768-well arrayed formats (82). These systems are increasingly used to screen compound libraries against ion channel targets, expediting the drug discovery process. However, the system requires a suspension of dissociated cells, which precludes recording in situ and over extended time courses. As a result, planar patch clamp is more suited for high-throughput screening of ion channel pharmacology than for analysis of cellular or tissue-level voltage signaling.

3.3.2. Nanopipettes and nanopillar electrodes.—The development of nanopipettes and nanopillar electrodes has enabled electrode-based access to broader length scales. Nanopipettes are a smaller version of sharp microelectrodes; their reduced size brings flexibility and access to small cellular compartments. Nanopipettes have been used to record from micron-scale dendritic spines, providing some of the first direct evidence for functional voltage compartmentalization in these structures (45). In addition, the flexibility of the nanopipette can stabilize in vivo recordings during animal behavior (46). As with sharp electrodes, the high tip resistances of the nanopipettes filter the signal and create a shunt that changes the observed V_{mem}, so the output signal must be processed to obtain accurate results. Nanopillar electrode arrays enable simultaneous intracellular recordings from many cells in a culture via a grid of nanoscale electrodes (94, 113). These platforms facilitate mapping of electrical activity across neuronal circuits or beating cardiomyocytes. However, the cells of interest must be cultured directly onto the electrode grid; nanopillar electrode arrays are not yet capable of in situ mapping of tissue V_{mem}. Overall, electrode engineering offers a promising avenue for increasing the spatial reach of electrophysiology.

4. CALIBRATED OPTICAL SIGNALS FOR RECORDING ABSOLUTE MEMBRANE POTENTIAL

A variety of optical V_{mem} measurement strategies use fluorescence as a proxy for V_{mem}, employing small-molecule or protein-based sensors engineered to display V_{mem}-sensitive fluorescence (Table 2). Optical platforms generally enjoy excellent spatial resolution, low invasiveness, and medium throughput. However, achieving the requisite temporal resolution, voltage resolution, and signal-to-noise ratio has required more engineering. Optical strategies fall into four categories (single-color intensity, ratio based, pump probe, and single-color lifetime; Figure 3). In all cases, rigorous calibration must be performed to relate the optical signal to the underlying absolute V_{mem}, which is most effectively achieved by performing the optical recording while V_{mem} is tuned across a range of known values. As we discuss in this section, a key difference among the various fluorescence-based strategies is voltage resolution, which is a result of the reproducibility of this calibration over time and between cells.

4.1. Strategies for Calibration of Optical Membrane Potential Reporters

To calibrate an optical V_{mem} recording platform, one must be able to measure the optical response across a range of V_{mem} values. By fitting this measured relationship to a function, one can then convert the optically determined parameter into V_{mem} values and, equally

importantly, estimate the accuracy of the optical V_{mem} determination. For example, for a linear relationship, one would determine the slope and the *y*-intercept and use those values to relate the optically recorded parameter to V_{mem}. To this end, there are three common strategies for setting cellular V_{mem}: electrode-based, pharmacological, and optogenetic.

4.1.1. Electrode-based calibration.—The most accurate method for calibrating fluorescence with respect to V_{mem} is whole-cell voltage clamp electrophysiology, which uses an intracellular recording configuration to inject current until the cell reaches the desired V_{mem}. The response across a range of precisely set V_{mem} can then be evaluated, determining the relationship between the optical readout and the underlying voltage. However, this approach is best when performed in isolated, single cells, and it suffers from the limitations of electrophysiology discussed above.

4.1.2. Pharmacological calibration.—If the system under study is inaccessible to electrode-based strategies, either pharmacology or intrinsic V_{mem} signals can be used to approximate the relationship between the optical signal and absolute V_{mem}. Reference values of V_{mem} have been established using ionophores for the primary ion establishing V_{mem} (39, 51, 74, 81), high extracellular K^+ (120–150 mM) (55, 74), and cell death or fixation with paraformaldehyde (PFA) (51). PFA and ionophores produce a more reliable 0-mV point than do high K^+ treatments, but they interact with the plasma membrane itself, which can change the fluorescence properties of the voltage sensor (79). Furthermore, there is no reliable way to access the sensitivity of the sensor (i.e., slope of signal versus V_{mem}) from a single pharmacological set point. However, in samples with well-described intrinsic electrical responses, a V_{mem} event of known magnitude can provide a standard for approximate determination of absolute V_{mem} sensitivity. Demonstrated reference V_{mem} signals include sustained hyperpolarization in Purkinje cells (19), depolarization resulting from glutamate uncaging (107), and back-propagating APs in dendrites (85). Such strategies are noninvasive but are limited to the small subset of samples where a useful and consistent V_{mem} signal can be identified.

4.1.3. Efforts toward optogenetic calibration.—In many cases, this limited set of calibration options is inadequate. Recently developed optical strategies for V_{mem} control may eventually provide an alternative to the above approaches, although they cannot yet tune V_{mem} to defined voltages. Engineering efforts for optical V_{mem} actuators have focused on channelrhodopsins, proteins that pass current in response to light. For setting V_{mem} optically, step-function opsins may be particularly useful, as they continue to pass current for minutes after initial activation (12, 119). Recently, light sensitivity was engineered into other ion channels via domain insertion, allowing diverse channels to serve as optogenetic actuators (27). These strategies could eventually allow precise setting of V_{mem} without an electrode.

4.2. Single-Color Fluorescence Intensity Recordings Are Difficult to Relate to Absolute Membrane Potential

In single-color fluorescence intensity–based recordings, V_{mem} affects the quantum yield or absorption coefficient of a sensor, producing changes in its fluorescence emission.

Fluorescence intensity of a voltage sensor in a membrane is recorded over seconds or minutes, enabling detection of V_{mem} changes and characterization of V_{mem} waveforms. A variety of sensor architectures have been documented (57, 77, 115, 116), including both small-molecule dyes and genetically encoded voltage indicators (GEVIs). Many sensors display sufficiently fast temporal resolution to follow millisecond-time APs. State-of-the-art systems can achieve cell-resolved recording of single APs in vivo from superficial brain regions, often with subcellular detail (1, 3, 88). However, single-color fluorescence intensity is best suited for V_{mem} event detection and generally cannot report absolute V_{mem}. Methods that rely solely on fluorescence intensity to monitor V_{mem} display large differences in baseline signal between cells and over minutes to hours. These variations are V_{mem} independent, arising from variable sensor loading or trafficking, cell morphology, sensor photobleaching, fluorescence quenching, and illumination intensity. As a result, calibrations made on one cell at a given time cannot be extended to other cells or even to the same cell hours later.

Fluorescence intensity:

the total amount of fluorescence signal from a sample; for fluorescent sensors, intensity depends on the amount of sensor present, the amount of light absorbed, and the quantum yield

Voltage indicator:

a small molecule or protein fluorophore that exhibits V_{mem} dependence in some or all of its fluorescent properties (e.g., intensity, wavelength, lifetime)

Some attempts have been made to calibrate fluorescence intensity to known V_{mem} at each cell or structure of interest, but caution must be employed in interpreting these results. Electrophysiological calibration of each individual cell is often challenging or impractical, so fluorescence intensity calibrations are generally performed with less accurate pharmacological strategies. In some cases, this approach is the only viable way to interrogate V_{mem}—for example, gramicidin-based calibrations and the V_{mem} indicator Archaerhodopsin (Arch) revealed subcellular differences in the AP waveform (39). However, pharmacological calibration of a single-color V_{mem} sensor is prone to artifacts. When calibrating from a single pharmacological set point, rather than a range of V_{mem} set by an electrode, the researcher must assume that the fractional change in fluorescence (%ΔF/F) per mV of the indicator is the same for all samples. In reality, the ΔF/F response to a given ΔV_{mem} will depend on the ratio of productively engaged sensor to background sensor, which may vary in space with trafficking or loading of the sensor. Furthermore, even with electrode-based calibration, many voltage sensors display sensitivity to membrane composition (36), which varies not only between cells but also within cells with complex membrane structures (10).

4.3. Ratio-Based Fluorescent Sensors Improve Reproducibility

Ratio-based voltage sensors show changes in the relative intensities of two fluorescence channels. The primary strategies for ratio-based fluorescent V_{mem} sensors rely on either Förster resonance energy transfer (FRET)-based indicators or electrochromic dyes. If the stoichiometry between the two signals is known, then the second channel can be used to correct for variability arising from cell morphology and dye loading. Ideally, the corrected signal would then be a stable proxy for absolute V_{mem} over time and across many cells without recalibration. In practice, ratio-based sensors achieve better absolute V_{mem} resolution than single-color intensity-based techniques, but they generally do not have sufficient resolution to quantify the biologically relevant V_{mem} differences between cells (~10–20 mV).

Ratio-based:

expressed as a ratio between two components; in ratio-based fluorescent imaging, the ratio of signal at two different wavelengths changes in response to the phenomenon of interest

4.3.1. Förster resonance energy transfer–based membrane potential sensors.—FRET-based V_{mem} sensors exhibit V_{mem}-dependent energy transfer from a donor to an acceptor fluorophore. Because the fluorescence intensities of the donor and acceptor are voltage sensitive in opposite directions, the ratio of the two can provide better fractional responses and a higher signal-to-noise ratio than a single color alone. Although a variety of FRET-based V_{mem} sensors exist, we are not aware of their use to document absolute V_{mem}, largely due to variable stoichiometry between the donor and acceptor. For genetically encoded systems (3, 4, 125), different rates of photobleaching, folding, and productive trafficking to the plasma membrane lead to variability in FRET ratios between cells. For small-molecule FRET-oxonol systems (15, 35), differences in loading between the two lipophilic indicators lead to variability in the %ΔF/F (72). As a result, FRET ratio measurements are not extensible between cells. Furthermore, the FRET-based reporters that undergo conformational changes to sense V_{mem} suffer from reduced temporal resolution and toxicity from capacitive load. In practice, these probes are primarily used to detect APs, with the second color serving to improve the signal-to-noise ratio or reduce motion artifacts.

4.3.2. Electrochromic ratio-based membrane potential sensors.—Electrochromic dyes, such as the ANEPPS (68) and ANNINE (34) classes, show V_{mem}-dependent excitation and/or emission spectra. A ratio signal is obtained by comparing the emission in a fixed band produced by excitation at two different wavelengths (or vice versa with a fixed excitation and two emission bands). Because electrochromic dyes are based on a charge shift mechanism, they have submillisecond temporal responses but display low sensitivity (~10% change per 100 mV) (33, 79). Normalized ANEPPS fluorescence ratios are accurate to approximately 5 mV for quantifying V_{mem} changes on an individual cell (17, 122). In combination with random access microscopy, di-8-ANEPPS ratios can report the AP waveform in absolute V_{mem} optically with excellent spatiotemporal resolution (exposure times of 0.5 ms and spatial resolution of 2 μm) (17). However, the V_{mem} calibration does not

translate between cells and must be performed with an electrode on each cell of interest to achieve this accuracy. The origin of the variability of the absolute ratio between cells is unclear; it likely depends on a complex combination of temperature, membrane composition, and probe loading.

4.3.3. Molecular beacons in ratio-based membrane potential recording.—

A recent, promising architecture for ratio-based V_{mem} sensors uses a molecular beacon, where the sensor contains one fluorophore that is voltage sensitive and a second fluorophore that is a voltage-independent reference. This strategy was tested with the GEVI Arch(D95N) fused to green fluorescent protein (GFP), but absolute V_{mem} quantification was not possible because of differential photobleaching of GFP and Arch(D95N) (41). More recently, the molecular beacon system was implemented with small-molecule V_{mem} sensors in Voltair (98), which comprises the VoltageFluor (VF) RVF5 (56) and the reference fluorophore ATTO647N on a DNA chassis. By normalizing the RVF5 signal to ATTO647N, Voltair was able to estimate organellar V_{mem} optically based on a pharmacological calibration, but absolute V_{mem} resolution of this technique has not yet been determined.

4.4. Pump-Probe Recordings: Accurate, with Complex Instrumentation

The temporal dynamics and vibrational signature of a probe do not depend on probe concentration; therefore, they can be used as a reproducible proxy for absolute V_{mem}. The temporal dynamics of the GEVI Arch(D95H)-eGFP can report absolute V_{mem} between cells with 10-mV resolution (41), the best yet reported for an optical system. However, access to and interpretation of such data is challenging for most laboratories, limiting this optical system's utility as a general V_{mem} sensing platform. Stimulated Raman scattering (SRS) has also been investigated as a strategy for absolute V_{mem} recordings, but its V_{mem} resolution has yet to be determined. Recently, the SRS signal of near-infrared opsins was shown to be sensitive to bulk depolarization in *Escherichia coli* membranes (61). Moreover, label-free detection of neuronal APs with SRS has been reported, although the mechanism of such V_{mem} sensitivity remains unclear (62). Further investigations of temporal dynamics and SRS as V_{mem} reporting platforms are of great interest, especially with the aim of translating them into more widely available systems.

4.5. Fluorescence Lifetime Offers Accessible Absolute Optical Membrane Potential Recordings

Fluorescence lifetime (τ_{fl}), or the amount of time that probe molecules remain in the fluorescent excited state, has recently garnered attention for its ability to report cellular properties (e.g., Ca^{2+} concentration or V_{mem}) absolutely using a single fluorescence channel (118). τ_{fl} is largely independent of fluorophore concentration, cellular morphology, and photobleaching, although it displays sensitivity to parameters such as temperature and viscosity. The primary downside to fluorescence lifetime imaging (FLIM) is its poor temporal resolution, with most acquisition times on the order of seconds.

Fluorescence lifetime (τ_{fl}):

the amount of time that a fluorophore remains in the fluorescent excited state before returning to the ground state, via either fluorescence ora nonradiative pathway

Fluorescence lifetime imaging (FLIM):

a microscopy technique in which both fluorescence intensity and τ_{fl} are recorded at each pixel of an image

4.5.1. Fluorescence lifetime of genetically encoded voltage indicators.— τ_{fl}-based V_{mem} recordings can be performed if τ_{fl} of a sensor changes reproducibly with V_{mem}. Many GEVIs sense V_{mem} through complex photocycles or multiple conformational states; this leads to low sensitivity in τ_{fl} or nonlinear relationships between τ_{fl} and V_{mem}. For example, the rhodopsin derivative Arch(D95H) was first evaluated in FLIM for its absolute V_{mem}-reporting capabilities, but its τ_{fl}–V_{mem} relationship was difficult to interpret (41). Comparison of the V_{mem} sensitivity of three GEVIs in two-photon illuminated FLIM (16) revealed that only CAESR (125) was suitable for absolute V_{mem} recording. CAESR exhibits 20-mV accuracy for quantifying V_{mem} changes on a given cell in a one-second bandwidth, but it displays too much variability to extend optical V_{mem} calibrations between cells (16). This between-cell variability may arise from the complex dynamics of rhodopsin fluorescence, coupled with intracellular fluorescence signal from incorrectly trafficked protein. V_{mem}-sensitive FLIM has also been demonstrated for FRET-oxonol V_{mem} sensors(31) and for accumulation-based sensors of mitochondrial potential (83), but no estimation of the absolute V_{mem} resolution was made in these systems.

4.5.2. Fluorescence lifetime of VoltageFluor small-molecule dyes.— τ_{fl}-based absolute V_{mem} imaging was developed further in our laboratory, achieving stable calibration between cells through the use of small-molecule VFs as voltage sensors. The voltage-sensing trigger for VFs is photoinduced electron transfer (78), which translates to a rapid, linear V_{mem} response in both fluorescence intensity (11, 78) and τ_{fl} (59). The τ_{fl} of VF2.1.Cl (VF-FLIM) can be calibrated to report absolute V_{mem} with a resolution of 5 mV for quantifying voltage changes on individual cells. These calibrations can be extended from one cell to another while retaining a single-trial V_{mem} resolution of 20 mV, which is sufficient to detect biologically relevant variation in resting V_{mem}, especially once multiple measurements are averaged. Because VF-FLIM calibrations are consistent for a given cell line, we were able to extend V_{mem} calibrations across thousands of cells after an initial electrode-based calibration on only a few cells. We applied VF-FLIM to study epidermal growth factor signaling and found a 15-mV hyperpolarizing response in carcinoma cells, showcasing its potential for elucidating diverse signaling roles of V_{mem}.

In addition to its improved V_{mem} resolution, VF-FLIM shows many promising attributes as a V_{mem} sensing platform. The increased stability of the calibration enhances throughput; an individual researcher using VF-FLIM could perform V_{mem} recordings at the speed of optical imaging (thousands of cells in an afternoon) rather than electrophysiology (~10 cells per day). Importantly, the temporal and spatial resolution of FLIM-based strategies are related:

Acquisition rates as fast as 200 Hz (exposures of 5 ms) can be obtained with reduced spatial resolution, and spatial resolution can be improved from 5 microns (the width of a binned pixel) to approximately 1 micron at the expense of imaging speed (Miller lab, unpublished data). The VF-FLIM technology can be further improved through combination with red-shifted V_{mem} sensors (28, 43) and targeting of sensors to specific cell populations in thick tissue (29, 67, 84), both of which are ongoing efforts in our lab. Overall, FLIM-based absolute V_{mem} imaging extends the timescale over which V_{mem} can be recorded and displays some of the best V_{mem} resolution to date for optical systems.

5. OUTLOOK

V_{mem} signals run the gamut from milliseconds to days and from the subcellular to the tissue level (Figure 1). The existing V_{mem} toolkit can record most cellular V_{mem} signals and some subcellular ones, with time resolutions ranging from milliseconds to minutes. V_{mem} signals delocalized across tissues are still challenging to interrogate, especially those occurring over hours to days.

Electrode-based absolute V_{mem} recordings have defined the field for years and will remain pivotal as engineering efforts continue to improve throughput and reduce invasiveness. However, progress in optical approaches for absolute V_{mem} recording has already expanded the range of space and time over which V_{mem} can be recorded. One of the key limitations to the scope of optical, absolute V_{mem} recording is the need for calibration in the cell or tissue of interest; we excitedly await improved optical actuators to facilitate V_{mem} calibrations in diverse systems. Further improvements in voltage-sensitive dyes and proteins stand to increase the absolute V_{mem} resolution of existing optical approaches. Improvements to photon-counting FLIM hardware, as well as fast frequency-domain FLIM strategies (91), are promising avenues for faster lifetime recordings. Optical V_{mem} recording in vivo can be multiplexed across more cells and larger areas by combining it with lattice light-sheet imaging (24) and other fast volumetric imaging strategies (50).

With these technological advances, we are constructing a picture of V_{mem} across biological time and space scales. Nevertheless, our atlas remains far from complete. In many cases, the information carried by V_{mem} is unknown, and the molecular mechanisms of V_{mem} response remain obfuscated. Each newly observed V_{mem} signal raises additional, exciting questions: How does the cell bring about these V_{mem} changes? Which molecules respond to V_{mem}? How are these signals transduced to downstream cellular processes? Uncovering the signaling networks surrounding V_{mem} will require platforms that interface with other cell profiling and omics techniques, such as the recently pioneered Patch-Seq system (18). With such efforts, we move ever closer to a systems-level understanding of V_{mem} in all of its diversity.

ACKNOWLEDGMENTS

The authors thank Holly Aaron and members of the Miller lab for helpful discussions. J.R.L.-D. was supported in part by a National Science Foundation Graduate Research Fellowship. A.M.M.G. was supported in part by a training grant from the National Institute of General Medical Sciences (NIGMS) (grant T32GM066698). E.W.M. acknowledges funding support from NIGMS (grant R35GM119855).

DISCLOSURE STATEMENT

E.W.M. is listed on a patent, owned by the Regents of the University of California, describing voltage-sensitive fluorophores. The other authors are not aware of any affiliations, memberships, funding, or financial holdings that might be perceived as affecting the objectivity of this review.

LITERATURE CITED

1. Abdelfattah AS, Kawashima T, Singh A, Novak O, Liu H, et al. 2019. Bright and photostable chemigenetic indicators for extended in vivo voltage imaging. Science 365(6454):699–704 [PubMed: 31371562]
2. Abdul Kadir L, Stacey M, Barrett-Jolley R. 2018. Emerging roles of the membrane potential: action beyond the action potential. Front. Physiol 9:1661 [PubMed: 30519193]
3. Adam Y, Kim JJ, Lou S, Zhao Y, Xie ME, et al. 2019. Voltage imaging and optogenetics reveal behaviour-dependent changes in hippocampal dynamics. Nature 569:413–17 [PubMed: 31043747]
4. Akemann W, Mutoh H, Perron A, Park YK, Iwamoto Y, Knopfel T. 2012. Imaging neural circuit dynamics with a voltage-sensitive fluorescent protein. J. Neurophysiol 108(8):2323–37 [PubMed: 22815406]
5. Alcamí P, Pereda AE. 2019. Beyond plasticity: the dynamic impact of electrical synapses on neural circuits. Nat. Rev. Neurosci 20(5):253–71 [PubMed: 30824857]
6. Arcangeli A, Bianchi L, Becchetti A, Faravelli L, Coronnello M, et al. 1995. A novel inward-rectifying K^+ current with a cell-cycle dependence governs the resting potential of mammalian neuroblastoma cells. J. Physiol 489(2):455–71 [PubMed: 8847640]
7. Armstrong CM, Gilly WF. 1992. Access resistance and space clamp problems associated with whole-cell patch clamping. Methods Enzymol. 207:100–22 [PubMed: 1528114]
8. Bean BP. 2007. The action potential in mammalian central neurons. Nat. Rev. Neurosci 8(6):451–65 [PubMed: 17514198]
9. Beaulieu-Laroche L, Toloza EHS, van der Goes MS, Lafourcade M, Barnagian D, et al. 2018. Enhanced dendritic compartmentalization in human cortical neurons. Cell 175(3):643–51.e14 [PubMed: 30340039]
10. Bedlack RS Jr., Wei MD, Fox SH, Gross E, Loew LM. 1994. Distinct electric potentials in soma and neurite membranes. Neuron 13(5):1187–93 [PubMed: 7946355]
11. Beier HT, Roth CC, Bixler JN, Sedelnikova AV, Ibey BL. 2019. Visualization of dynamic sub-microsecond changes in membrane potential. Biophys. J 116(1):120–26 [PubMed: 30579565]
12. Berndt A, Yizhar O, Gunaydin LA, Hegemann P, Deisseroth K. 2009. Bi-stable neural state switches. Nat. Neurosci 12(2):229–34 [PubMed: 19079251]
13. Bi G, Poo M. 2001. Synaptic modification by correlated activity: Hebb's postulate revisited. Annu. Rev. Neurosci 24:139–66 [PubMed: 11283308]
14. Brette R, Destexhe A. 2012. Intracellular recording. In Handbook of Neural Activity Measurement, ed. Brette R, pp. 44–91. Cambridge, UK: Cambridge Univ. Press
15. Briggman KL, Kristan WB, González JE, Kleinfeld D, Tsien RY. 2010. Monitoring integrated activity of individual neurons using FRET-based voltage-sensitive dyes. In Membrane Potential Imaging in the Nervous System: Methods and Applications, ed. Canepari M, Zecevic D, pp. 61–70. Berlin: Springer
16. Brinks D, Klein AJ, Cohen AE. 2015. Two-photon lifetime imaging of voltage indicating proteins as a probe of absolute membrane voltage. Biophys. J 109(5):914–21 [PubMed: 26331249] Compared the performance of three GEVIs in reporting absolute V_{mem} under two-photon illumination.
17. Bullen A, Saggau P. 1999. High-speed, random-access fluorescence microscopy: II. Fast quantitative measurements with voltage-sensitive dyes. Biophys. J 76(4):2272–87 [PubMed: 10096922] Combined random-access imaging with electrochromic dyes to quantify V_{mem} along neurons with high spatiotemporal resolution.
18. Cadwell CR, Palasantza A, Jiang X, Berens P, Deng Q, et al. 2016. Electrophysiological, transcriptomic and morphologic profiling of single neurons using Patch-seq. Nat. Biotechnol

34(2):199–203 [PubMed: 26689543] Characterized the transcriptomic basis of morphological and electrical signatures of diverse neurons.

19. Canepari M, Vogt K, Zecevic D. 2008. Combining voltage and calcium imaging from neuronal dendrites. Cell. Mol. Neurobiol 28(8):1079–93 [PubMed: 18500551]
20. Cang C, Bekele B, Ren D. 2014. The voltage-gated sodium channel TPC1 confers endolysosomal excitability. Nat. Chem. Biol 10(6):463–69 [PubMed: 24776928]
21. Ceriani F, Mammano F. 2013. A rapid and sensitive assay of intercellular coupling by voltage imaging of gap junction networks. Cell Commun. Signal 11(1):78 [PubMed: 24144139]
22. Cervera J, Alcaraz A, Mafe S. 2016. Bioelectrical signals and ion channels in the modeling of multicellular patterns and cancer biophysics. Sci. Rep 6:20403 [PubMed: 26841954]
23. Cervera J, Meseguer S, Mafe S. 2016. The interplay between genetic and bioelectrical signaling permits a spatial regionalisation of membrane potentials in model multicellular ensembles. Sci. Rep 6:35201 [PubMed: 27731412]
24. Chen BC, Legant WR, Wang K, Shao L, Milkie DE, et al. 2014. Lattice light-sheet microscopy: imaging molecules to embryos at high spatiotemporal resolution. Science 346(6208):1257998 [PubMed: 25342811]
25. Chen L, Becker TM, Koch U, Stauber T. 2019. The LRRC8/VRAC anion channel facilitates myogenic differentiation of murine myoblasts by promoting membrane hyperpolarization. J. Biol. Chem 294:14279–88 [PubMed: 31387946]
26. Cone CD, Cone CM. 1976. Induction of mitosis in mature neurons in central nervous system by sustained depolarization. Science 192(4235):155–58 [PubMed: 56781]
27. Coyote-Maestas W, He Y, Myers CL, Schmidt D. 2019. Domain insertion permissibility-guided engineering of allostery in ion channels. Nat. Commun 10:290 [PubMed: 30655517]
28. Deal PE, Kulkarni RU, Al-Abdullatif SH, Miller EW. 2016. Isomerically pure tetramethylrhodamine voltage reporters. J. Am. Chem. Soc 138(29):9085–88 [PubMed: 27428174]
29. Deal PE, Liu P, Al-Abdullatif SH, Muller VR, Shamardani K, et al. 2020. Covalently tethered rhodamine voltage reporters for high speed functional imaging in brain tissue. J. Am. Chem. Soc 142(1):614–22 [PubMed: 31829585]
30. Delling M, Decaen PG, Doerner JF, Febvay S, Clapham DE. 2013. Primary cilia are specialized calcium signalling organelles. Nature 504(7479):311–14 [PubMed: 24336288] Showed that primary cilia are electrically compartmentalized, with distinct Ca^{2+} levels and V_{mem}.
31. Dumas D, Stoltz JF. 2005. New tool to monitor membrane potential by FRET voltage sensitive dye (FRET-VSD) using spectral and fluorescence lifetime imaging microscopy (FLIM): interest in cell engineering. Clin. Hemorheol. Microcirc 33(3):293–302 [PubMed: 16215295]
32. Fertig N, Blick RH, Behrends JC. 2002. Whole cell patch clamp recording performed on a planar glass chip. Biophys. J 82(6):3056–62 [PubMed: 12023228]
33. Fluhler E, Burnham VG, Loew LM. 1985. Spectra, membrane binding, and potentiometric responses of new charge shift probes. Biochemistry 24(21):5749–55 [PubMed: 4084490]
34. Fromherz P, Hübener G, Kuhn B, Hinner MJ. 2008. ANNINE-6plus, a voltage-sensitive dye with good solubility, strong membrane binding and high sensitivity. Eur. Biophys. J 37(4):509–14 [PubMed: 17687549]
35. Gonzalez JE, Tsien RY. 1997. Improved indicators of cell membrane potential that use fluorescence resonance energy transfer. Chem. Biol 4(4):269–77 [PubMed: 9195864]
36. Gross E, Bedlack RS, Loew LM. 1994. Dual-wavelength ratiometric fluorescence measurement of the membrane dipole potential. Biophys. J 67(1):208–16 [PubMed: 7918989]
37. Holcman D, Yuste R. 2015. The new nanophysiology: regulation of ionic flow in neuronal subcompartments. Nat. Rev. Neurosci 16(11):685–92 [PubMed: 26462753]
38. Holst GL, Stoy W, Yang B, Kolb I, Kodandaramaiah SB, et al. 2019. Autonomous patch-clamp robot for functional characterization of neurons in vivo: development and application to mouse visual cortex. J. Neurophysiol 121(6):2341–57 [PubMed: 30969898]
39. Hoppa MB, Gouzer G, Armbruster M, Ryan TA. 2014. Control and plasticity of the presynaptic action potential waveform at small CNS nerve terminals. Neuron 84(4):778–89 [PubMed: 25447742]

40. Horn R, Marty A. 1988. Muscarinic activation of ionic currents measured by a new whole-cell recording method. J. Gen. Physiol 92(2):145–59 [PubMed: 2459299]
41. Hou JH, Venkatachalam V, Cohen AE. 2014. Temporal dynamics of microbial rhodopsin fluorescence reports absolute membrane voltage. Biophys. J 106(3):639–48 [PubMed: 24507604] Reported absolute V_{mem} with 10-mV resolution using temporal dynamics of the GEVI Arch(D95H).
42. Huang X, Jan LY. 2014. Targeting potassium channels in cancer. J. Cell Biol 206(2):151–62 [PubMed: 25049269]
43. Huang YL, Walker AS, Miller EW. 2015. A photostable silicon rhodamine platform for optical voltage sensing. J. Am. Chem. Soc 137(33):10767–76 [PubMed: 26237573]
44. Jacquemet G, Baghirov H, Georgiadou M, Sihto H, Peuhu E, et al. 2016. L-type calcium channels regulate filopodia stability and cancer cell invasion downstream of integrin signalling. Nat. Commun 7:13297 [PubMed: 27910855]
45. Jayant K, Hirtz JJ, Plante IJ-L, Tsai DM, De Boer WDAM, et al. 2017. Targeted intracellular voltage recordings from dendritic spines using quantum-dot-coated nanopipettes. Nat. Nanotechnol 12(4):335–42 [PubMed: 27941898] Developed nanopipettes capable of recording from dendritic spines and demonstrated spine electrical compartmentalization.
46. Jayant K, Wenzel M, Bando Y, Hamm JP, Mandriota N, et al. 2019. Flexible nanopipettes for minimally invasive intracellular electrophysiology in vivo. Cell Rep. 26(1):266–78.e5 [PubMed: 30605681]
47. Johri A, Beal MF. 2012. Mitochondrial dysfunction in neurodegenerative diseases. J. Pharmacol. Exp. Ther 342(3):619–30 [PubMed: 22700435]
48. Kasper EM, Larkman AU, Lübke J, Blakemore C. 1994. Pyramidal neurons in layer 5 of the rat visual cortex. II. Development of electrophysiological properties. J. Comp. Neurol 339(4):475–94 [PubMed: 8144742]
49. Kato K, Clifford DB, Zorumski CF. 1993. Long-term potentiation during whole-cell recording in rat hippocampal slices. Neuroscience 53(1):39–47 [PubMed: 8097020]
50. Kazemipour A, Novak O, Flickinger D, Marvin JS, Abdelfattah AS, et al. 2019. Kilohertz frame-rate two-photon tomography. Nat. Methods 16(8):778–86 [PubMed: 31363222]
51. Klapperstück T, Glanz D, Klapperstück M, Wohlrab J. 2009. Methodological aspects of measuring absolute values of membrane potential in human cells by flow cytometry. Cytom. A 75(7):593–608
52. Kodandaramaiah SB, Franzesi GT, Chow BY, Boyden ES, Forest CR. 2012. Automated whole-cell patch-clamp electrophysiology of neurons in vivo. Nat. Methods 9(6):585–87 [PubMed: 22561988]
53. Kole MHP, Stuart GJ. 2012. Signal processing in the axon initial segment. Neuron 73(2):235–47 [PubMed: 22284179]
54. Korn SJ, Horn R. 1989. Influence of sodium-calcium exchange on calcium current rundown and the duration of calcium-dependent chloride currents in pituitary cells, studied with whole cell and perforated patch recording. J. Gen. Physiol 94(5):789–812 [PubMed: 2556494]
55. Krasznai Z, Márián T, Balkay L, Emri M, Trón L. 1995. Flow cytometric determination of absolute membrane potential of cells. J. Photochem. Photobiol. B 28(1):93–99 [PubMed: 7791010]
56. Kulkarni RU, Kramer DJ, Pourmandi N, Karbasi K, Bateup HS, Miller EW. 2017. Voltage-sensitive rhodol with enhanced two-photon brightness. PNAS 114(11):2813–18 [PubMed: 28242676]
57. Kulkarni RU, Miller EW. 2017. Voltage imaging: pitfalls and potential. Biochemistry 56(39):5171–77 [PubMed: 28745864]
58. Larkin J, Garcia-Ojalvo J, Prindle A, Liu J, Gabalda-Sagarra M, et al. 2017. Coupling between distant biofilms and emergence of nutrient time-sharing. Science 356(6338):638–42 [PubMed: 28386026]
59. Lazzari-Dean JR, Gest AMM, Miller EW. 2019. Optical estimation of absolute membrane potential using fluorescence lifetime imaging. eLife 8:e44522 [PubMed: 31545164] Demonstrated that the fluorescence lifetime of VFs reports absolute V_{mem} with high resolution and improved throughput.

60. Lee DD, Galera-Laporta L, Bialecka-Fornal M, Moon EC, Shen Z, et al. 2019. Magnesium flux modulates ribosomes to increase bacterial survival. Cell 177(2):352–60 [PubMed: 30853217]
61. Lee HJ, Huang K-C, Mei G, Zong C, Mamaeva N, et al. 2019. Electronic preresonance stimulated Raman scattering imaging of red-shifted proteorhodopsins: toward quantitation of the membrane potential. J. Phys. Chem. Lett 10(15):4374–81 [PubMed: 31313926]
62. Lee HJ, Zhang D, Jiang Y, Wu X, Shih P-Y, et al. 2017. Label-free vibrational spectroscopic imaging of neuronal membrane potential. J. Phys. Chem. Lett 8(9):1932–36 [PubMed: 28407470]
63. LeSauter J, Silver R, Cloues R, Witkovsky P. 2011. Light exposure induces short- and long-term changes in the excitability of retinorecipient neurons in suprachiasmatic nucleus. J. Neurophysiol 106(2):576–88 [PubMed: 21593396]
64. Levin M 2014. Molecular bioelectricity: how endogenous voltage potentials control cell behavior and instruct pattern regulation in vivo. Mol. Biol. Cell 25(24):3835–50 [PubMed: 25425556]
65. Li W-C, Soffe SR, Roberts A. 2004. A direct comparison of whole cell patch and sharp electrodes by simultaneous recording from single spinal neurons in frog tadpoles. J. Neurophysiol 92(1):380–86 [PubMed: 14999043]
66. Linley JE. 2013. Perforated whole-cell patch-clamp recording. In Ion Channels: Methods and Protocols, ed. Gamper N, pp. 149–57. Berlin: Springer
67. Liu P, Grenier V, Hong W, Muller VR, Miller EW. 2017. Fluorogenic targeting of voltage-sensitive dyes to neurons. J. Am. Chem. Soc 139(48):17334–40 [PubMed: 29154543]
68. Loew LM, Scully S, Simpson L, Waggoner AS. 1979. Evidence for a charge-shift electrochromic mechanism in a probe of membrane potential. Nature 281(5731):497–99 [PubMed: 492309]
69. Loewenstein WR, Kanno Y. 1964. Studies on an epithelial (gland) cell junction I. Modifications of surface membrane permeability. J. Cell Biol 22:565–86 [PubMed: 14206423]
70. Low BC, Pan CQ, Shivashankar GV, Bershadsky A, Sudol M, Sheetz M. 2014. YAP/TAZ as mechanosensors and mechanotransducers in regulating organ size and tumor growth. FEBS Lett. 588(16):2663–70 [PubMed: 24747426]
71. Magni M, Meldolesi J, Pandiella A. 1991. Ionic events induced by epidermal growth factor: evidence that hyperpolarization and stimulated cation influx play a role in the stimulation of cell growth. J. Biol. Chem 266(10):6329–35 [PubMed: 1706715]
72. Maher MP, Wu NT, Ao H. 2007. pH-insensitive FRET voltage dyes. J. Biomol. Screen 12(5):656–67 [PubMed: 17517905]
73. Malinow R, Tsien RW. 1990. Presynaptic enhancement shown by whole-cell recordings of long-term potentiation in hippocampal slices. Nature 346(5429):177–80 [PubMed: 2164158]
74. Maric D, Maric I, Smith SV, Serafini R, Hu Q, Barker JL. 1998. Potentiometric study of resting potential, contributing K^+ channels and the onset of Na^+ channel excitability in embryonic rat cortical cells. Eur. J. Neurosci 10(8):2532–46 [PubMed: 9767384]
75. McCormick DA, Prince DA. 1987. Post-natal development of electrophysiological properties of rat cerebral cortical pyramidal neurones. J. Physiol 393(1):743–62 [PubMed: 2895811]
76. McNamara HM, Salegame R, Al Tanoury Z, Xu H, Begum S, et al. 2020. Bioelectrical domain walls in homogeneous tissues. Nat. Phys 16(3):357–64 [PubMed: 33790984] Provided theoretical and direct experimental evidence for stable V_{mem} patterning in tissue.
77. Miller EW. 2016. Small molecule fluorescent voltage indicators for studying membrane potential. Curr. Opin. Chem. Biol 33:74–80 [PubMed: 27318561]
78. Miller EW, Lin JY, Frady EP, Steinbach PA, Kristan WB, Tsien RY. 2012. Optically monitoring voltage in neurons by photo-induced electron transfer through molecular wires. PNAS 109(6):2114–19 [PubMed: 22308458]
79. Montana V, Farkas DL, Loew LM. 1989. Dual-wavelength ratiometric fluorescence measurements of membrane potential. Biochemistry 28(11):4536–39 [PubMed: 2765500]
80. Murata Y, Iwasaki H, Sasaki M, Inaba K, Okamura Y. 2005. Phosphoinositide phosphatase activity coupled to an intrinsic voltage sensor. Nature 435(7046):1239–43 [PubMed: 15902207]
81. Novo D, Perlmutter NG, Hunt RH, Shapiro HM. 1999. Accurate flow cytometric membrane potential measurement in bacteria using diethyloxacarbocyanine and a ratiometric technique. Cytometry 35(1):55–63 [PubMed: 10554181]

82. Obergrussberger A, Brüggemann A, Goetze TA, Rapedius M, Haarmann C, et al. 2016. Automated patch clamp meets high-throughput screening: 384 cells recorded in parallel on a planar patch clamp module. J. Lab. Autom 21(6):779–93 [PubMed: 26702021]
83. Okkelman IA, Papkovsky DB, Dmitriev RI. 2020. Estimation of the mitochondrial membrane potential using fluorescence lifetime imaging microscopy. Cytom. A 97(5):471–82
84. Ortiz G, Liu P, Naing SHH, Muller VR, Miller EW. 2019. Synthesis of sulfonated carbofluoresceins for voltage imaging. J. Am. Chem. Soc 141(16):6631–38 [PubMed: 30978010]
85. Palmer LM, Stuart GJ. 2009. Membrane potential changes in dendritic spines during action potentials and synaptic input. J. Neurosci 29(21):6897–903 [PubMed: 19474316]
86. Pandiella A, Magni M, Lovisolo D, Meldolesi J. 1989. The effects of epidermal growth factor on membrane potential. J. Biol. Chem 264(22):12914–21 [PubMed: 2787795]
87. Perkins KL. 2006. Cell-attached voltage-clamp and current-clamp recording and stimulation techniques in brain slices. J. Neurosci. Methods 154(1–2):1–18 [PubMed: 16554092]
88. Piatkevich KD, Jung EE, Straub C, Linghu C, Park D, et al. 2018. A robotic multidimensional directed evolution approach applied to fluorescent voltage reporters. Nat. Chem. Biol 14(4):352–60 [PubMed: 29483642]
89. Prindle A, Liu J, Asally M, Ly S, Garcia-Ojalvo J, et al. 2015. Ion channels enable electrical communication in bacterial communities. Nature 527(7576):59–63 [PubMed: 26503040]
90. Rad MS, Cohen LB, Braubach O, Baker BJ. 2018. Monitoring voltage fluctuations of intracellular membranes. Sci. Rep 8:6911 [PubMed: 29720664]
91. Raspe M, Kedziora KM, van den Broek B, Zhao Q, de Jong S, et al. 2016. siFLIM: Single-image frequency-domain FLIM provides fast and photon-efficient lifetime data. Nat. Methods 13(6):501–4 [PubMed: 27088314]
92. Rinne A, Birk A, Bünemann M. 2013. Voltage regulates adrenergic receptor function. PNAS 110(4):1536–41 [PubMed: 23297214]
93. Rinne A, Mobarec JC, Mahaut-Smith M, Kolb P, Bünemann M. 2015. The mode of agonist binding to a G protein-coupled receptor switches the effect that voltage changes have on signaling. Sci. Signal 8(401):ra110 [PubMed: 26535008]
94. Robinson JT, Jorgolli M, Shalek AK, Yoon MH, Gertner RS, Park H. 2012. Vertical nanowire electrode arrays as a scalable platform for intracellular interfacing to neuronal circuits. Nat. Nanotechnol 7(3):180–84 [PubMed: 22231664]
95. Rohr S 2004. Role of gap junctions in the propagation of the cardiac action potential. Cardiovasc. Res 62(2):309–22 [PubMed: 15094351]
96. Rolfe DFS, Brown GC. 1997. Cellular energy utilization and molecular origin of standard metabolic rate in mammals. Physiol. Rev 77(3):731–58 [PubMed: 9234964]
97. Sada N, Lee S, Katsu T, Otsuki T, Inoue T. 2015. Targeting LDH enzymes with a stiripentol analog to treat epilepsy. Science 347(6228):1362–67 [PubMed: 25792327]
98. Saminathan A, Devany J, Veetil AT, Suresh B, Pillai KS, et al. 2021. A DNA-based voltmeter for organelles. Nat. Nanotechnol 16(1):96–103 [PubMed: 33139937]
99. Sánchez A, Urrego D, Pardo LA. 2016. Cyclic expression of the voltage-gated potassium channel KV10.1 promotes disassembly of the primary cilium. EMBO Rep. 17(5):708–23 [PubMed: 27113750]
100. Sigworth FJ, Neher E. 1980. Single Na^+ channel currents observed in cultured rat muscle cells. Nature 287:447–49 [PubMed: 6253802]
101. Spruston N, Johnston D. 1992. Perforated patch-clamp analysis of the passive membrane properties of three classes of hippocampal neurons. J. Neurophysiol 67(3):508–29 [PubMed: 1578242]
102. Stuart GJ, Spruston N. 2015. Dendritic integration: 60 years of progress. Nat. Neurosci 18(12):1713–21 [PubMed: 26605882]
103. Suk HJ, van Welie I, Kodandaramaiah SB, Allen B, Forest CR, Boyden ES. 2017. Closed-loop real-time imaging enables fully automated cell-targeted patch-clamp neural recording in vivo. Neuron 95(5):1037–47.e11 [PubMed: 28858614]

104. Tsuchiya W, Okada Y. 1982. Membrane potential changes associated with differentiation of enterocytes in the rat intestinal villi in culture. Dev. Biol 94(2):284–90 [PubMed: 6295851]
105. Tyzio R, Ivanov A, Bernard C, Holmes GL, Ben-Ari Y, Khazipov R. 2003. Membrane potential of CA3 hippocampal pyramidal cells during postnatal development. J. Neurophysiol 90:2964–72 [PubMed: 12867526] Revealed discrepancies in V_{mem} as reported by whole-cell, cell-attached, and perforated-patch recordings.
106. Verheugen JA, Fricker D, Miles R. 1999. Noninvasive measurements of the membrane potential and GABAergic action in hippocampal interneurons. J. Neurosci 19(7):2546–55 [PubMed: 10087068]
107. Vogt KE, Gerharz S, Graham J, Canepari M. 2011. Combining membrane potential imaging with lglutamate or GABA photorelease. PLOS ONE 6(10):e24911 [PubMed: 22022367]
108. Wang SY, Melkoumian Z, Woodfork KA, Cather C, Davidson AG, et al. 1998. Evidence for an early G1 ionic event necessary for cell cycle progression and survival in the MCF-7 human breast carcinoma cell line. J. Cell. Physiol 176(3):456–64 [PubMed: 9699498]
109. White TW, Paul DL. 1999. Genetic diseases and gene knockouts reveal diverse connexin functions. Annu. Rev. Physiol 61:283–310 [PubMed: 10099690]
110. Williams SR, Mitchell SJ. 2008. Direct measurement of somatic voltage clamp errors in central neurons. Nat. Neurosci 11(7):790–98 [PubMed: 18552844]
111. Wonderlin WF, Woodfork KA, Strobl JS. 1995. Changes in membrane potential during the progression of MCF-7 human mammary tumor cells through the cell cycle. J. Cell. Physiol 165(1):177–85 [PubMed: 7559799]
112. Wu J, Lewis AH, Grandl J. 2017. Touch, tension, and transduction—the function and regulation of piezo ion channels. Trends Biochem. Sci 42(1):57–71 [PubMed: 27743844]
113. Xie C, Lin Z, Hanson L, Cui Y, Cui B. 2012. Intracellular recording of action potentials by nanopillar electroporation. Nat. Nanotechnol 7(3):185–90 [PubMed: 22327876] Constructed nanopillar electrode arrays for intracellular recording of action potentials from many neurons over days.
114. Xu H, Martinoia E, Szabo I. 2015. Organellar channels and transporters. Cell Calcium 58(1):1–10 [PubMed: 25795199]
115. Xu Y, Zou P, Cohen AE. 2017. Voltage imaging with genetically encoded indicators. Curr. Opin. Chem. Biol 39:1–10 [PubMed: 28460291]
116. Yang HH, St-Pierre F. 2016. Genetically encoded voltage indicators: opportunities and challenges. J. Neurosci 36(39):9977–89 [PubMed: 27683896]
117. Yang M, Brackenbury WJ. 2013. Membrane potential and cancer progression. Front. Physiol 4:185 [PubMed: 23882223]
118. Yellen G, Mongeon R. 2015. Quantitative two-photon imaging of fluorescent biosensors. Curr. Opin. Chem. Biol 27:24–30 [PubMed: 26079046]
119. Yizhar O, Fenno LE, Prigge M, Schneider F, Davidson TJ, et al. 2011. Neocortical excitation/inhibition balance in information processing and social dysfunction. Nature 477(7363):171–78 [PubMed: 21796121]
120. Yuste R 2013. Electrical compartmentalization in dendritic spines. Annu. Rev. Neurosci 36:429–49 [PubMed: 23724997]
121. Zhang J, Chen X, Xue Y, Gamper N, Zhang X. 2018. Beyond voltage-gated ion channels: voltage-operated membrane proteins and cellular processes. J. Cell. Physiol 233(10):6377–85 [PubMed: 29667735]
122. Zhang J, Davidson RM, Wei MD, Loew LM. 1998. Membrane electric properties by combined patch clamp and fluorescence ratio imaging in single neurons. Biophys. J 74(1):48–53 [PubMed: 9449308]
123. Zhou Y, Wong C, Cho K, van der Hoeven D, Liang H, et al. 2015. Membrane potential modulates plasma membrane phospholipid dynamics and K-Ras signaling. Science 349(6250):873–76 [PubMed: 26293964]
124. Zorova LD, Popkov VA, Plotnikov EY, Silachev DN, Pevzner IB, et al. 2018. Mitochondrial membrane potential. Anal. Biochem 552:50–59 [PubMed: 28711444]

125. Zou P, Zhao Y, Douglass AD, Hochbaum DR, Brinks D, et al. 2014. Bright and fast multicoloured voltage reporters via electrochromic FRET. Nat. Commun 5:4625 [PubMed: 25118186]

SUMMARY POINTS

1. V_{mem} influences cellular processes on timescales ranging from seconds to days and across length scales from microns to centimeters. Beyond excitable cell APs, V_{mem} also contributes to cell growth, differentiation, and organellar function.
2. V_{mem} recording strategies generally fall into one of two categories: electrode-based or optical recordings.
3. Electrode-based V_{mem} recordings have high temporal resolution and voltage resolution, but they are invasive, have low throughput, and only record V_{mem} at a single point.
4. Recent advances in electrodes and electrode arrays have allowed for electrophysiology of smaller cellular structures, as well as improved throughput and multiplexing.
5. Optical V_{mem} recordings can track V_{mem} noninvasively across many cells at once, but most optical strategies cannot quantify biologically relevant V_{mem} signals (i.e., measure absolute V_{mem}).
6. Recent improvements in certain optical V_{mem} recording platforms have improved V_{mem} resolution, thereby enabling quantification of absolute V_{mem}. In particular, lifetime or temporal dynamics of a sensor's fluorescence can quantify V_{mem} across longer space and timescales.
7. Optical recordings are indirect measurements of V_{mem}, so they always require calibration to report absolute V_{mem}. Various optical V_{mem} recording architectures show differences in the reproducibility of this calibration; this is usually the limiting factor in absolute V_{mem} resolution.

FUTURE ISSUES

1. Many areas of V_{mem} biology are understudied, especially V_{mem} changes occurring over long periods of time and in very small or very large structures. Continued efforts toward developing platforms for absolute V_{mem} recordings are necessary before we can fully document or understand V_{mem} signaling in these areas.
2. Electrical signaling in vivo is likely delocalized across multiple cells by gap junctions. As tools tailored to measure V_{mem} in tissue are developed, further investigations into cell–cell coupling and long-range V_{mem} signals are needed.
3. Absolute V_{mem} recording platforms with signals that are stable over days are needed. Although nanopillar electrode arrays are a major step forward, electrode-based platforms are generally too invasive for chronic recordings. A key challenge for optical platforms is maintaining stable levels of V_{mem} sensor in the sample during extended recordings.
4. Standard metrics for—and routine determination of—absolute V_{mem} resolution should be incorporated into the evaluation and presentation of optical platforms for quantitative V_{mem} recordings (ratio-based recordings, lifetime-based recordings, SRS, etc.).
5. More generalizable strategies for calibration of V_{mem} are needed. In systems that are accessible optically but not with electrodes, it is difficult to determine the accuracy of optical absolute V_{mem} measurements.
6. Although FLIM and temporal dynamics–based strategies have accessed resolutions in the range of 10–20 mV, many interesting V_{mem} changes are on the scale of 5–10 mV. Further engineering of these optical sensors and platforms could enable detection of subtle V_{mem} changes.

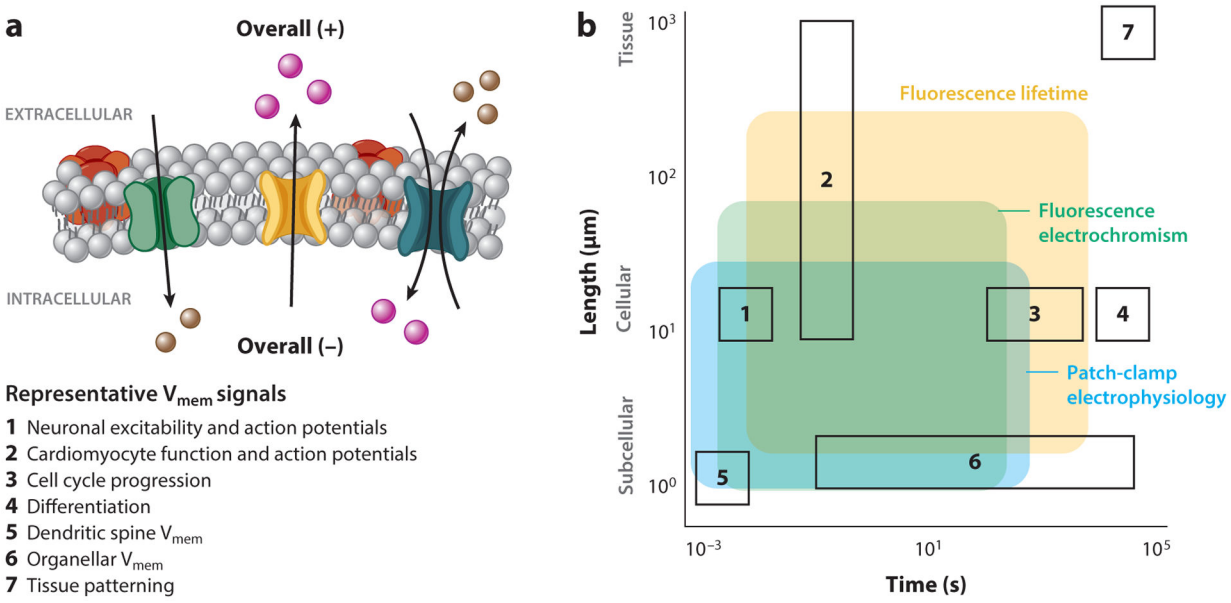

Figure 1.

Membrane potential (V_{mem}) signals and measurement techniques across time and space. (*a*) A schematic of cellular V_{mem}, with examples of seven biological processes where V_{mem} signaling plays a role. The resistance to ionic flow between compartments sets the length scale of V_{mem} signals; V_{mem} can scale across tissues or be compartmentalized within organelles or dendritic spines. The properties of ion channels and pumps that determine V_{mem}, as well as ion diffusion between compartments, dictate the time duration of a V_{mem} response. (*b*) Biological space accessible to the three most common strategies for absolute V_{mem} measurement (*shaded regions*), overlaid with example biological process of interest (*outlined boxes*, numbered as in panel *a*). While many techniques can report cellular V_{mem} on the scale of milliseconds or seconds, longer recordings or recordings across large areas are difficult to access. Shaded areas indicate regions where single trial recordings retain voltage resolution on the scale of biological V_{mem} changes (≤20 mV) and minimally alter the biological sample. Recordings with fluorescence electrochromic dyes require recalibration with an electrode on each cell, whereas fluorescence lifetime and patch-clamp electrophysiology can be applied as stand-alone measurements that are comparable between cells. Shaded areas are restricted to demonstrated application space for each technique and do not indicate the full extent of its possible use.

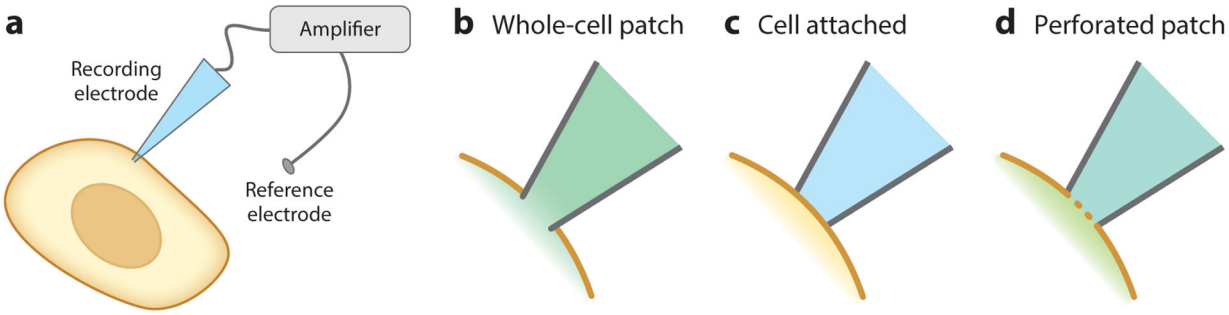

Figure 2.

Electrophysiological configurations for V_{mem} recording. (*a*) General schematic for electrode-based V_{mem} recordings, in which a cell comes into direct contact with an electrode. Voltage is measured as the difference between the recording electrode and a reference electrode in the bath solution. (*b–d*) Close-up of the interface between the membrane and the electrode in different electrophysiology configurations. (*b*) In whole-cell patch-clamp electrophysiology, the plasma membrane is ruptured, and the cytosol mixes with the recording electrode solution. (*c*) In the cell-attached configuration, the plasma membrane is left intact. (*d*) In perforated patch, the membrane is not ruptured, but ionophores introduced into the recording solution allow ionic exchange across the membrane.

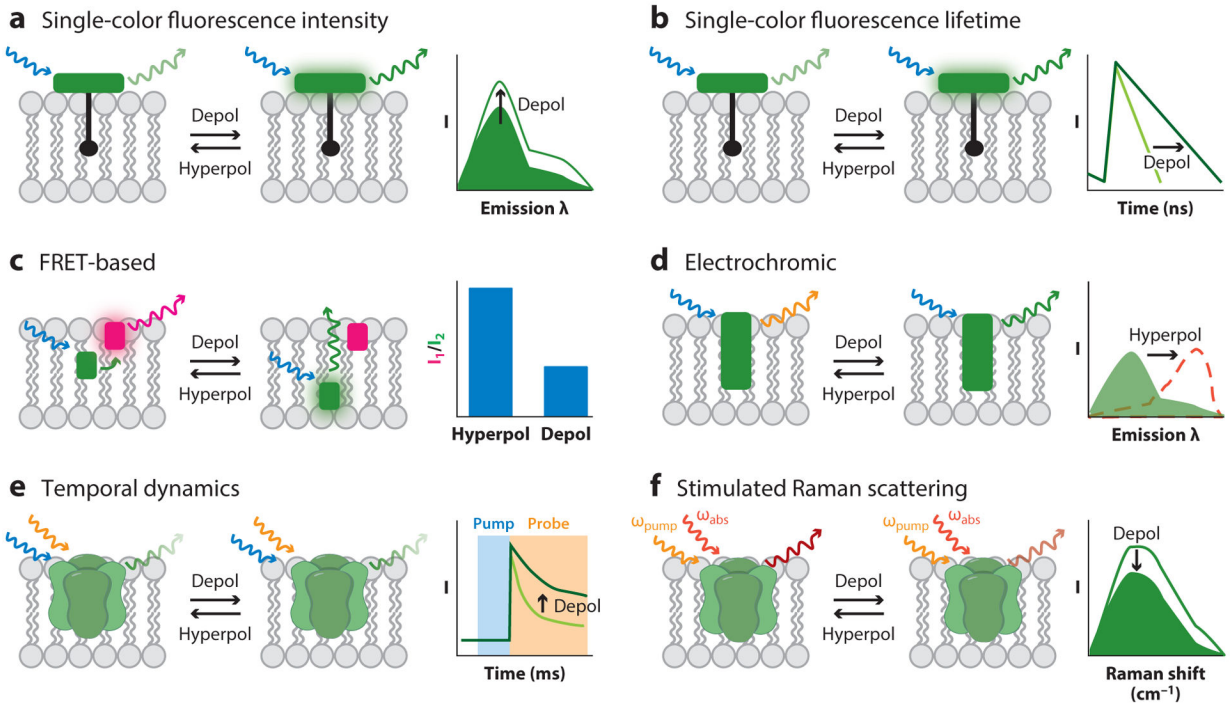

Figure 3.

Optical strategies for reporting absolute V_{mem}. (*a*) Single-color fluorescence intensity recordings detect changes in V_{mem} by changes in a sensor's fluorescence quantum yield (shown), extinction coefficient, or cellular concentration. This technique generally cannot report absolute V_{mem} optically, although estimates can be made if calibrations are performed for every cell of interest. (*b*) Single-color fluorescence lifetime can report absolute V_{mem}, particularly if the V_{mem} sensor operates via photoinduced electron transfer.(*c*) FRET-based sensors show differences in the FRET ratios of two fluorophores, often resulting from V_{mem}-dependent changes in the distance between the two. The diagram shows a FRET-oxonol system. (*d*) The excitation and/or emission spectra of electrochromic dyes depend on the electric field in the plasma membrane. (*e*) Certain GEVIs show V_{mem}-related differences in the temporal dynamics of the absorption of their excited state. (*f*) SRS imaging reports changes in V_{mem}-dependent vibrational frequencies. Abbreviations:λ, wavelength; depol, depolarization; FRET, Förster resonance energy transfer; GEVI, genetically encoded voltage indicator; hyperpol, hyperpolarization; SRS, stimulated Raman scattering; V_{mem}, membrane potential.

Table 1

Comparison of electrode-based V_{mem} recording strategies

Performance attribute	Whole-cell patch clamp[a]	Cell attached[b]	Perforated patch[c]	Nanopipettes[d]	Nanopillars[e]	Planar patch clamp[f]
Spatial resolution	– (single point)	– (single point)	– (single point)	– (single point)	++ (grid of points)	– (single point)
Temporal resolution	+++ (μs–ms)	+++ (μs–ms)	+++ (μs–ms)	+++ (μs–ms)	+++ (μs–ms)	+++ (μs–ms)
Voltage resolution	+++ (1 mV)	+ (variable)	+++ (1 mV)	+++ (1 mV)	+++ (1 mV)	+++ (1 mV)
Stability	+ (mins–1 h)	+ (mins–1 h)	++ (~1 h)	+ (mins–1 h)	+++ (days)	+ (mins–1 h)
Noninvasiveness	−	++	+	+	+	–
In situ capabilities	++	++	++	++	–	–
Access to subcellular structures	+	+	+	+++	++	–
Throughput and multiplexing	–	–	–	–	++	+++
Ease of use	–	–	–	–	+	++

[a] Described in References 7, 14, 38, 49, 52, 73, 100, 103, 105, and 110.

[b] Described in References 87, 105, and 106.

[c] Described in References 40, 54, and 66.

[d] Described in References 45 and 46.

[e] Described in References 94 and 113.

[f] Described in References 32 and 82.

Technique performance in each category is ranked as follows: −, poor; +, fair; ++, good; +++, excellent. Abbreviation: V_{mem}, membrane potential.

Table 2

Comparison of optical V_{mem} recording strategies

Performance attribute	Single-color fluorescence intensity[a]	Single-color fluorescence lifetime[b]	FRET-based[c]	Electrochromic (ratio-based)[d]	GEVI temporal dynamics[e]	Stimulated Raman scattering[f]
Spatial resolution[g]	+++ (<1 μm)	++ (~1 μm)[h]	+++ (<1 μm)	+++ (<1 μm)	++ (~1 μm)[h]	+ (>1 μm)[h]
Temporal resolution	++ (1 ms)	+ (5 ms)[h]	+ (1 ms or >10 ms)[i]	++ (1 ms)	– (s)[h]	++ (1 ms)[h]
Voltage resolution[j]	– (≫00 mV)	++ (VF: 20 mV, GEVI: >100 mV)	ND	+ (~100 mV)	++ (10 mV)	ND
Stability	+ (minutes)	++ (hours)	++ (hours)	+ (minutes)	ND	ND
Noninvasiveness	+++	+++	+++	+++	+++	+++
In situ capabilities	+++	+++	+++	+++	+++	++
Access to subcellular structures[k]	++	++	++	++	++	++
Throughput and multiplexing	+++	++	+++	+++	+	++
Ease of use	+++	+	++	++	–	–

[a] Many single-color fluorescence intensity V_{mem} sensors have been designed, although they are seldom used for absolute V_{mem} quantification. Data are compiled from References 57, 77, 115, and 116.

[b] Single-color fluorescence lifetime recordings have been shown for genetically encoded voltage indicators (16) and for small-molecule VFs (59).

[c] FRET-based systems may use conformational changes of the indicator (4), changes in the absorption spectrum of a rhodopsin derivative (3, 125), or translocation of charged groups in the membrane (15, 35, 72) to report V_{mem}. Many properties are similar across these architectures; metrics in this case represent all types of FRET-based strategies unless otherwise noted.

[d] Performance metrics are aggregated from References 17, 33, 34, 68, 79, and 122.

[e] Demonstrated in Reference 41.

[f] Demonstrated in References 61 and 62.

[g] Spatial resolution is determined by the diffraction limit, as well as optics used in the microscope. Techniques rated ++ rather than +++ generally require moderate spatial binning to obtain adequate signal.

[h] For fluorescence lifetime, GEVI temporal dynamics, and stimulated Raman scattering measurements, there is a trade-off between spatial and temporal resolution, and one may be sacrificed to improve the other. We list the best values of either spatial or temporal resolution shown in the literature or that we have demonstrated in our laboratory.

[i] FRET sensors based on protein conformational changes or dye translocation exhibit temporal resolution of >10 ms, whereas electrochromic FRET-based sensors can resolve millisecond-time V_{mem} events.

[j] Voltage resolution listed is for applying a calibration determined on one cell onto another individual cell; more precise V_{mem} measurements can be obtained if measurements from multiple cells are averaged. Most techniques have substantially better resolution for quantifying the magnitude of a V_{mem} change on an individual cell (e.g., VF-FLIM has 5-mV resolution for quantifying V_{mem} changes on a single cell versus 20-mV resolution for quantifying absolute V_{mem} alone).

[k] Limited by delivery of sensor to intracellular structures and/or the ability to isolate signal from only the subcellular membrane structure of interest when all membrane structures are stained.

Technique performance in each category is ranked as follows: −, poor; +, fair; ++, good; +++, excellent. Abbreviations: FLIM, fluorescence lifetime imaging; FRET, Förster resonance energy transfer; GEVI, genetically encoded voltage indicator; ND, not determined; VF, VoltageFluor; V_{mem}, membrane potential.